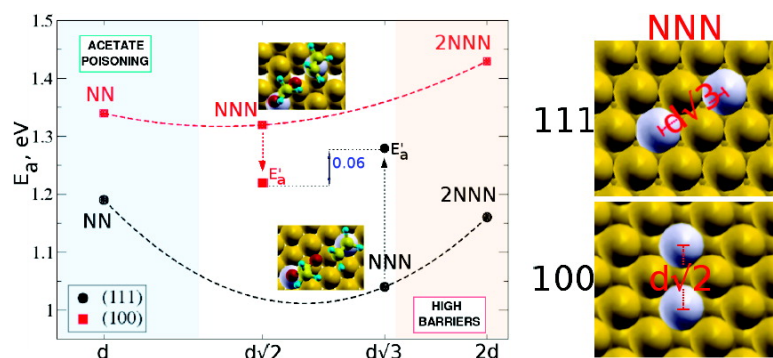


Template Effects in Vinyl Acetate Synthesis on PdAu Surface Alloys: A Density Functional Theory Study

Mo#nica García-Mota, and Nu#ria Lo#pez

J. Am. Chem. Soc., 2008, 130 (44), 14406-14407 • DOI: 10.1021/ja805519v • Publication Date (Web): 08 October 2008

Downloaded from <http://pubs.acs.org> on February 8, 2009



More About This Article

Additional resources and features associated with this article are available within the HTML version:

- Supporting Information
- Access to high resolution figures
- Links to articles and content related to this article
- Copyright permission to reproduce figures and/or text from this article

[View the Full Text HTML](#)

Template Effects in Vinyl Acetate Synthesis on PdAu Surface Alloys: A Density Functional Theory Study

Mónica García-Mota and Núria López*

Institute of Chemical Research of Catalonia, ICIQ, Avda. Països Catalans 16, 43007 Tarragona, Spain

Received July 16, 2008; E-mail: nlopez@icq.es

Vinyl acetate (VA) is a major industrial product involved in the manufacture of polymers. It is synthesized from the coupling of acetic acid and ethylene in oxygen ambient. Recently, isolated Pd dimers on Au surfaces have been found to be active and selective catalysts for the process but a strong dependence on the local structure of the ensemble is observed.¹ By means of density functional theory (DFT), we demonstrate how the most successful ensemble shows the best performance on different steps: easy adsorption of reactants, inhibited poisoning and low barrier for the rate limiting step (rls).

PdAu alloys have been revealed as new, powerful catalysts with applications in chemical and electrochemical contexts.^{1,2} In particular, low Pd content PdAu surface alloys show an intrinsic high activity and pronounced structure sensitivity toward the production of VA.¹ Vinyl acetate synthesis proceeds via the oxygen-assisted dissociative adsorption of acetic acid followed by the coupling to ethylene.³ The resulting intermediate, hydrogenated VA, (VAH in the following) evolves via β -hydrogen elimination to VA and a water molecule. This mechanism was determined both experimentally⁴ and theoretically,⁵ and the acetate-to-ethylene coupling was found to be the rls for Pd(100) and second nearest neighbors Pd on Au(100). However, the pronounced structure sensitivity found in the experiments^{1a} cannot be understood without considering the reaction path in a full set of local structures, and this is the precise aim of our study. More generally, ensemble effects are mandatory to reach an atomistic design of new catalysts. In the following, we employ DFT to determine what drives the structure sensitivity observed for the formation of VA on different ensembles of PdAu.

To this end we have built several Pd dimer configurations on both Au(100) and (111) (see Figure 1). To obtain the reaction profiles on the Pd dimers, the VASP code has been employed⁸ with RPBE as the exchange-correlation functional.⁹ Valence mono-electronic states have been expanded in plane waves with a kinetic cutoff energy of 400 eV while the inner electrons have been represented by PAW pseudopotentials.¹⁰ The slabs contain five layers for the (100) and four for the (111) surface in a $p(4 \times 4)$ supercell, and the slabs are interleaved by 12 Å of vacuum. On these surfaces two Au atoms have been replaced by Pd atoms in the configurations shown in Figure 1. Therefore, the Pd–Pd distances range from $d_{\text{Pd-Pd}}$ to twice this value. The configurations have been named as nearest neighbors: NN for the $d_{\text{Pd-Pd}}$ distance; next-nearest neighbors: NNN, $d\sqrt{2}$ or $d\sqrt{3}$ (for (100) and (111) surfaces, respectively); second next nearest neighbors: 2NNN, $2d$. The k -point sampling consists of $2 \times 2 \times 1$ Monkhorst–Pack points.¹¹ The two surface upper layers and the adsorbates have been optimized while the lowest layers were kept frozen at the bulk distances. With this setup, the relative energies to the most stable dimer for each surface are reported, see Figure 1. All these configurations are likely to be present on the samples at 0.1 ML Pd coverage on Au in agreement with previous experimental and theoretical results.^{1,2a,6,7} The CI-NEB method has been employed¹²

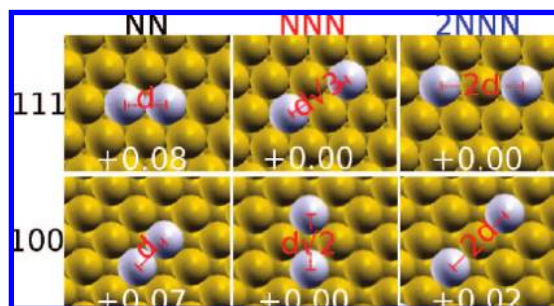


Figure 1. Dimer ensembles showing different local configurations on (111) and (100) Au surfaces. Yellow spheres represent Au, and gray ones are Pd atoms. NN stands for nearest neighbors, NNN next nearest neighbors, and 2NNN second next nearest neighbors. The numbers indicate the relative energies, in eV, to the most stable dimer on each surface. The interdimer distance is expressed in $d_{\text{Pd-Pd}}$ units.

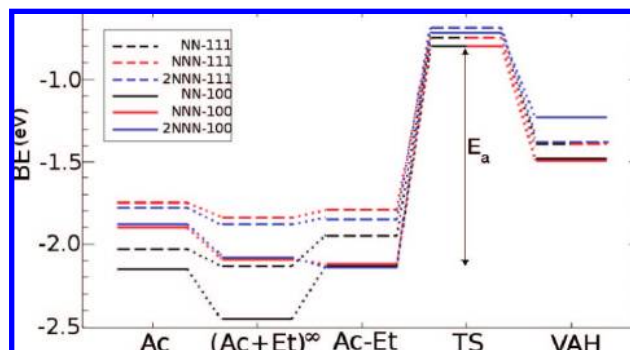


Figure 2. Reaction energy profiles, BE in eV (with respect to gas-phase acetate radical, ethylene, and the clean surface), for the coupling of ethylene and acetate on the models of Figure 1. Ac states for acetate, Et for ethylene, and the infinite sign represents separated adsorption. The structures for coadsorbed Ac–Et, the intermediate VAH, and the transition state linking both can be found in the Supporting Information.

to locate the transition-state structures (showing a single imaginary frequency), see Supporting Information.

The binding energies of reactants and intermediates, BE, (with respect to gas-phase acetate radical, ethylene, and the clean surface) are shown in Figure 2 together with the barriers for the rls. Binding energies to (111) surfaces are lower than those to (100), as expected from the d -band model.¹³ Adsorbed species can be classified according to their coordination to the surface (hapticity), $\eta^X_{\text{A},\dots}$, where X indicates the number of atoms through which the adsorbate is bound to the surface and “A,...” represents these atoms.

Ethylene is weakly adsorbed to the Pd dimers, through a π –Pd bond⁵ ca. -0.2 for (100) to ca. -0.1 eV for the (111) surfaces. Similarly, low binding energies have been found for ethylene on Ag.¹⁴ Acetate can be adsorbed either as monospecies or dihapto-species depending on the Pd ensemble, see Supporting Informa-

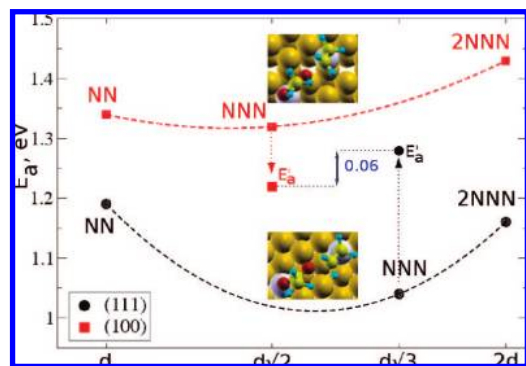


Figure 3. Activation energies, E_a in eV, for the rate limiting step, as a function of the template Pd–Pd distance. For the NNN dimers the apparent activation energies, E_a' , are also indicated. The insets show the transition state structures for NNN.

tion. For both surface orientations, acetate adsorption on NN templates results in dihapto- $\eta^2_{O,O}$ species ($BE = -2.15$ (100), -2.03 (111) eV) while for NNN and 2NNN monohaptospecies, $\eta^1_{O,O}$, are more stable ($BE \approx -1.90$ (100), -1.75 (111) eV).

The formation of the coadsorbed state (Ac–Et) requires the approach of both acetate and ethylene adsorbates to neighboring Pd atoms in the dimer. The NN configurations on both (111) and (100) pay an energy penalty, about 0.3 eV, for changing the configuration of the acetate from the dihapto in the infinitely separated configuration to the monohapto adsorption needed to generate the active complex (Ac–Et). For NNN and 2NNN the process is almost thermoneutral, ± 0.06 eV. In fact, strong bonding of the acetate- $\eta^2_{O,O}$ species to the NN ensemble results in poisoning of these templates under normal conditions.

The VAH intermediate bonds the dimers in a dihapto- $\eta^2_{O,C}$ mode by the terminal O and C atoms to the Pd. The binding energies of these species are very similar for all dimers on the (111) surface: -1.3 to 1.4 eV. For the (100) surface, adsorption energies are more spread: -1.49 , -1.44 , and -1.23 eV for NNN, NN, and 2NNN, respectively. Upon VAH dehydrogenation the vinyl acetate product is easily desorbed from the surface on both (111) and (100) surfaces (not shown in Figure 2).

To shed light on the structure sensitivity, we have calculated the barriers connecting the coadsorbed state (Ac–Et) and the VAH intermediate. All the barriers, E_a , range in between 1.04 and 1.43 eV. From the (Ac–Et) on the different dimers the energy barrier, E_a , follows a Brønsted–Evans–Polanyi (BEP)-type of relationship with the reaction energy,¹⁵ see Supporting Information. This means that the less endothermic the reaction is, the lower the barrier results. The reasons for the increased barriers at longer/shorter distances are mainly due to the energy cost of either the repulsion in the coadsorbed state structure or the strain/stress in the final VAH state.

The next step is to determine why in the experiments the NNN-(100) structures are more reactive than the corresponding (111). To understand the relative activity of NNN dimers all the elementary steps previous to the rate limiting step have to be taken into account and contribute to the apparent activation energy, E_a' . Working out the kinetic equations in the nearly empty surface approximation and considering constant preexponential factors,¹⁶ E_a' can be written as: $E_a' = E_a + \sum_i \Delta E_i$ where ΔE_i corresponds to the reaction energies of the previous steps in the reaction network. Those steps are oxygen

dissociation, oxygen assisted acetic acid adsorption, ethylene adsorption, and acetate ethylene approach. When E_a' are compared, the value for NNN(100) is 0.06 eV lower than that of the (111) surface. The reason for the lower E_a' in (100) comes from the better adsorption of reactants. This difference in apparent activation energies, $\Delta E_a' = E_a'^{100} - E_a'^{111}$, corresponds to a relative reaction rate at the experimental temperature (453 K)^{1a} of about 4–5 times faster for the (100) structure. This is in excellent agreement with experiments where the relative activities found at the (100) curve maximum are $r_{100}/r_{111} \approx 4.6$.^{1a}

To summarize, the structure sensitivity for the synthesis of VA on Pd dimers on PdAu surface alloys depends on three effects. First, electronic contributions that favor the reaction on the most open surface due to better adsorption of reactants. Second, the most successful ensemble, NNN, avoids poisoning by acetate adsorption due to template effects that block the formation of the dihaptoacetate species. Third, the Pd template induces small changes, in the structure and energies, of the coadsorbed structure and the VAH product by strain/stress effects,¹⁷ thus affecting the reaction barrier for the coupling step. These contributions follow a BEP type of relationship. A final remark is that the role of Au in these alloys is as a spacer isolating the Pd ensembles.

Acknowledgment. ICIQ, MEC (Consolider Ingenio 2010 CSD2006-003, CTQ2006-00464BQU), GenCat, and RES-CesViMa are acknowledged for support.

Supporting Information Available: Structures, imaginary frequencies, reaction energies and kinetic analysis are reported. This material is available free of charge via the Internet at <http://pubs.acs.org>.

References

- (1) (a) Chen, M. S.; Kumar, D.; Yi, C. W.; Goodman, D. W. *Science* **2005**, *310*, 291. (b) Kumar, D.; Chen, M. S.; Goodman, D. W. *Catal. Today* **2007**, *123*, 77. (c) Chen, M. S.; Luo, K.; Wei, T.; Yan, Z.; Kumar, D.; Yi, C. W.; Goodman, D. W. *Catal. Today* **2006**, *117*, 37.
- (2) (a) Maroun, F.; Ozanam, F.; Magnussen, O. M.; Behm, R. J. *Science* **2001**, *293*, 1811. (b) Enache, D. I.; Edwards, J. K.; Landon, P.; Solsona-Espriu, B.; Carley, A. F.; Herzing, A. A.; Watanabe, M.; Kiely, C. J.; Knight, D. W.; Hutchings, G. J. *Science* **2006**, *311*, 362.
- (3) Samanos, B.; Boutry, P.; Montarnal, R. *J. Catal.* **1971**, *23*, 19.
- (4) Stacchiola, D.; Calaza, F.; Burkholder, L.; Schwabacher, A. W.; Neurock, M.; Tyscoe, W. T. *Angew. Chem., Int. Ed.* **2005**, *44*, 4572.
- (5) Yuan, D. W.; Gong, X. G.; Wu, R. Q. *J. Phys. Chem. C* **2008**, *112*, 1539.
- (6) Han, P.; Axnanda, S.; Lyubinetsky, I.; Goodman, D. W. *J. Am. Chem. Soc.* **2007**, *129*, 14355. (b) Wei, T.; Wang, J.; Goodman, D. W. *J. Phys. Chem. C* **2007**, *111*, 8781.
- (7) (a) Liu, P.; Nørskov, J. K. *Phys. Chem. Chem. Phys.* **2001**, *3*, 3814. (b) Martin, R.; Takehiro, N.; Liu, P.; Nørskov, J. K.; Behm, R. J. *Chem. Phys. Chem.* **2007**, *8*, 2068. (c) Soto-Verdugo, V.; Metiu, H. *Surf. Sci.* **2007**, *62*, 4744. (d) Boscoboinik, J. A.; Plaisance, C.; Neurock, M.; Tyscoe, W. T. *Phys. Rev. B* **2008**, *77*, 045422.
- (8) (a) Kresse, G.; Hafner, J. *Phys. Rev. B* **1993**, *47*, 558. (b) Kresse, G.; Furthmüller, J. *Phys. Rev. B* **1996**, *54*, 11169.
- (9) Hammer, B.; Hansen, L. B.; Nørskov, J. K. *Phys. Rev. B* **1999**, *59*, 7413.
- (10) Kresse, G.; Joubert, D. *Phys. Rev. B* **1999**, *59*, 1758.
- (11) Monkhorst, H. J.; Pack, J. D. *Phys. Rev. B* **1976**, *13*, 5188.
- (12) Henkelman, G.; Uberuaga, B. P.; Jónsson, H. *J. Chem. Phys.* **2000**, *113*, 9901.
- (13) Hammer, B.; Morikawa, Y.; Nørskov, J. K. *Phys. Rev. Lett.* **1996**, *76*, 2141.
- (14) Bocquet, M. L.; Rappe, A. M.; Dai, H. L. *Mol. Phys.* **2005**, *103*, 883.
- (15) (a) Brønsted, J. N. *Chem. Rev.* **1928**, *5*, 231. (b) Evans, M. G.; Polanyi, M. *Transactions of Faraday Soc.* **1938**, *34*, 11. (c) Logadottir, A.; Rod, T. H.; Nørskov, J. K.; Hammer, B.; Dahl, S.; Jacobsen, C. J. H. *J. Catal.* **2001**, *197*, 229.
- (16) See Supporting Information and: Chorkendorff, I.; Niemantsverdriet, J. W. *Concepts of Modern Catalysis and Kinetics*; Wiley-VCH: Weinheim, Germany, 2003; Chapter 3 and p 38.
- (17) Mavrikakis, M.; Hammer, B.; Nørskov, J. K. *Phys. Rev. Lett.* **1998**, *81*, 2819.

JA805519V